Perioperative Precision Medicine
ISSN: 2957-5443

Review Article https://doi.org/10.61189/295165xbmhth

Limb nerve block localization using deep learning-driven segmentation: A review

Jiaxun Jiang[1], Miao Zhou[2], Liangqing Lin[3], Haipo Cui[1], Long Liu[1], Jiaen Wu[1], Zhaopeng Zhou[1]

[1]School of Health Science and Engineering, University of Shanghai for Science and Technology, Shanghai 200093, China. [2]Jiangsu Cancer Hospital, Nanjing 213164, Jiangsu Province, China. [3]Anesthesiology, The First Hospital of Putian, Putian 351100, Fujian Province, China.

Corresponding author: Haipo Cui.

Declaration of conflict of interest: None.

Received April 1, 2025; Accepted May 12, 2025; Published December 31, 2025

Highlights

- Deep learning-powered nerve block segmentation significantly contributes to optimized perioperative pain management by enhancing the precision and safety of regional anesthesia.
- Advanced architectures, particularly U-Net variants, dominate peripheral nerve block segmentation, offering high precision and adaptability to medical imaging challenges.
- Deep learning enhances clinical workflows by improving segmentation accuracy and efficiency in upper and lower limb nerve blocks, thereby supporting procedural success.
- Future efforts will focus on improving model robustness and generalizability to address limitations such as data variability and limited adaptability, facilitating broader clinical adoption.

Abstract

Effective pain management is a cornerstone of optimal perioperative care, significantly impacting patient recovery and outcomes. Regional anesthesia, particularly peripheral nerve blocks, plays a crucial role in achieving this by providing targeted analgesia. While ultrasound guidance has enhanced the precision of these procedures, challenges persist in accurately identifying nerve structures due to inherent image quality issues. Addressing these challenges is critical for improving the efficacy and safety of nerve blocks. Recent years have witnessed significant advances in medical image processing powered by deep learning, particularly in the segmentation of peripheral nerve blocks. This review summarizes current research progress and emerging techniques in this domain. We first introduce commonly used segmentation models, including Fully Convolutional Networks, U-Net and its variants, and task-specific network architectures. We then examine the application of deep learning to the segmentation of upper and lower limb nerve blocks, highlighting improvements in accuracy and efficiency. Current limitations-such as challenges with data heterogeneity and model generalization-are critically analyzed, and future directions are proposed to enhance model robustness and clinical scalability. Ultimately, this paper underscores the potential of deep learning to revolutionize peripheral nerve block localization through automated and reliable image segmentation.

Keywords: Deep learning, medical image processing, nerve block, perioperative medical applications

Introduction

Perioperative management is central to modern surgical practice, aiming to optimize the patient's overall experience and recovery before, during, and after surgery. Within this continuous process, effective pain management is a crucial component for ensuring patient comfort, accelerating postoperative recovery, and reducing complications. By precisely controlling post-

Address correspondence to: Haipo Cui, School of Health Science and Engineering, University of Shanghai for Science and Technology, No. 516 Jungong Road, Yangpu District, Shanghai 200093, China. E-mail: h_b_cui@163.com.

operative pain, patients can ambulate earlier, reduce hospital stays, and significantly improve their quality of life. To achieve this goal, regional anesthesia techniques, particularly nerve blocks, have become an essential part of perioperative pain management.

Nerve block procedures involve the precise injection of anesthetic agents around target nerves to interrupt neural conduction, providing local anesthesia or analgesia. These techniques are fundamental in clinical anesthesia and pain management [1]. Ultrasound guidance has become the standard approach for performing nerve blocks, offering significant advantages such as real-time visualization of nerves and surrounding structures. This facilitates more accurate needle placement and markedly improves procedural success rates and safety compared to traditional landmark-based methods [2]. However, ultrasound imaging is inherently challenged by issues such as noise, artifacts, speckle patterns, and often indistinct or blurred nerve boundaries, making accurate interpretation difficult [3]. These limitations highlight the need for advanced auxiliary technologies to assist clinicians in reliably identifying nerve structures.

Computer-aided analysis, particularly medical image segmentation, plays a pivotal role in the quantitative assessment of images from various modalities [4, 5]. Early segmentation approaches primarily relied on traditional image processing techniques, including edge-based, region-based, and threshold-based methods [6-8]. While these methods achieved limited success, their performance is significantly constrained by the variability and quality limitations inherent in medical imaging, often proving inadequate for achieving reliable segmentation in real-world clinical settings [9].

The rapid advancement of computer vision and machine learning—especially the rise of deep learning (DL)—has revolutionized medical image segmentation [10]. Convolutional Neural Networks (CNNs), in particular, have demonstrated outstanding performance in segmentation tasks and now represent the predominant methodology in this field. Compared to traditional approaches, CNNs offer distinct advantages such as automatic hierarchical feature extraction, robustness to image variability, and high segmentation accuracy [11]. For example, Wu et al. developed a CNNs model that successfully segmented the brachial plexus in ultrasound images captured at oblique angles [12]. The model achieved a mean Dice coefficient of 0.748 and a mean Jaccard index of 0.630, demonstrating superior resilience to noise and blurred boundaries compared to conventional methods, and showing effective nerve delineation at the interscalene level.

These strengths have led to the widespread adoption of DL in medical image analysis, significantly advancing computer-aided diagnosis and intervention planning—particularly for the complex task of interpreting ultrasound images. Applying these advanced segmentation techniques to ultrasound-guided peripheral nerve blocks holds significant clinical promise: enhancing block success rates and safety, reducing complications, and improving patient comfort.

This review provides a comprehensive overview of DL-based image segmentation techniques and their specific applications in identifying peripheral nerves in ultrasound images for nerve block procedures. The article is organized as follows: First, we introduce mainstream DL segmentation methods relevant to this field. Next, we discuss their application and performance in ultrasound-guided peripheral nerve blocks. Finally, we analyze current advantages and limitations and explore future directions, including the potential for clinical integration of ultrasound-assisted nerve identification technologies.

Image segmentation techniques

Fully convolutional networks (FCNs)

FCNs represent a pivotal advancement in DL, primarily applied to semantic image segmentation. First introduced by Long et al. in 2015, FCNs addressed the limitations of traditional CNNs in segmentation tasks by proposing a new approach for pixel-level classification [13]. Traditional CNNs typically employ fully connected layers at their final stages to produce fixed-size outputs, which are insufficient for segmentation tasks requiring detailed spatial localization.

FCNs overcome this limitation by replacing fully connected layers with convolutional and

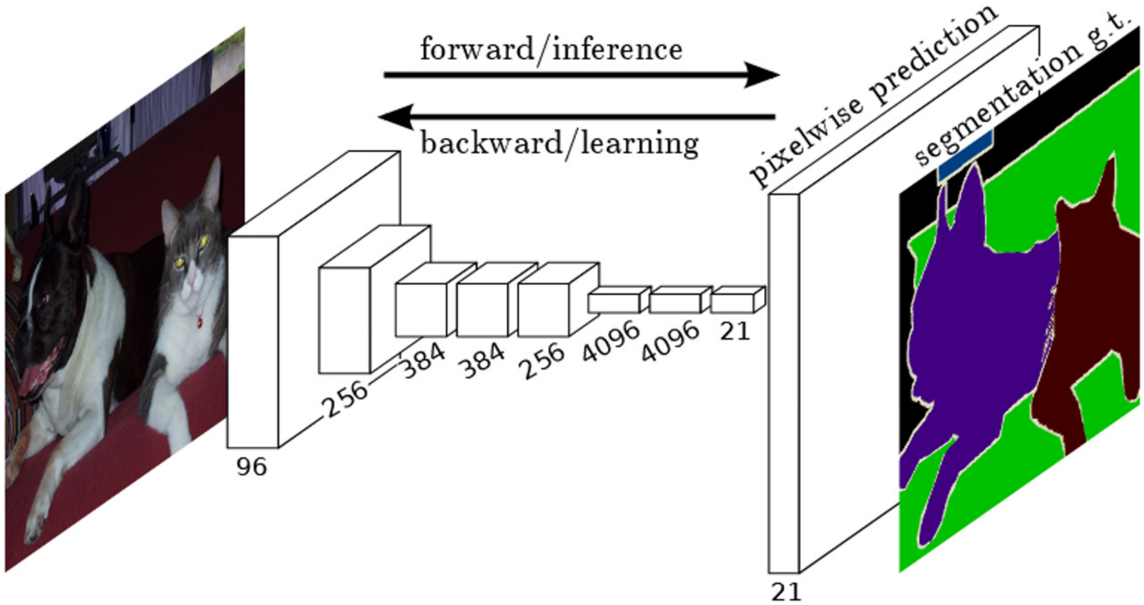

Figure 1. The Fundamental Architecture of FCNs. This figure was cited from [13]. FCNs, Fully Convolutional Networks.

upsampling layers, enabling dense, pixel-wise predictions while preserving spatial hierarchies. By integrating multi-scale feature representations, FCNs achieve fine-grained segmentation performance across various domains. The fundamental architecture of an FCNs is illustrated in **Figure 1**.

To tackle the challenges of low accuracy and long processing times in medical ultrasound segmentation, a team of researchers proposed a multi-scale dilated convolution approach based on an improved FCNs [7]. Their method employed image preprocessing to enhance input quality, constructed four dilated convolutional layers with different dilation rates to fuse contextual information across scales, and utilized Laplacian-based post-processing to refine segmentation boundaries. Experiments showed substantial improvement in segmentation accuracy on breast ultrasound datasets, particularly in fuzzy and structurally complex regions.

Huang et al. introduced an FCNs architecture augmented with attention modules to enhance semantic segmentation performance [14]. By integrating skip-layer and post-processing attention mechanisms, the model strengthened feature dependencies and improved adaptability to complex backgrounds. Their model achieved state-of-the-art performance on several public datasets.

Miao et al. developed an FCNs variant using dilated convolutions to expand the receptive field of convolutional kernels, thereby enhancing the network's ability to capture fine neural structures [15]. This model demonstrated superior performance in segmenting peripheral nerve block images, notably improving both segmentation accuracy and contrast.

FCNs have been widely applied in nerve block image segmentation, enabling precise nerve localization, real-time guidance, automation, and improved procedural efficiency. Their clinical utility lies in reducing physician workload and enhancing surgical outcomes [16]. However, FCNs are computationally demanding, especially when handling high-resolution medical images. They also tend to struggle with capturing extremely fine structures due to resolution limitations [17].

U-Net architecture and its variants

U-Net is a DL architecture specifically designed for image segmentation and has shown exceptional performance in medical image analysis. Introduced by Ronneberger et al. in 2015, U-Net was developed to address the limitations of traditional segmentation techniques, especially in applications with small training Datasets [18].

The U-Net architecture features a symmetric U-shaped design composed of two main paths:

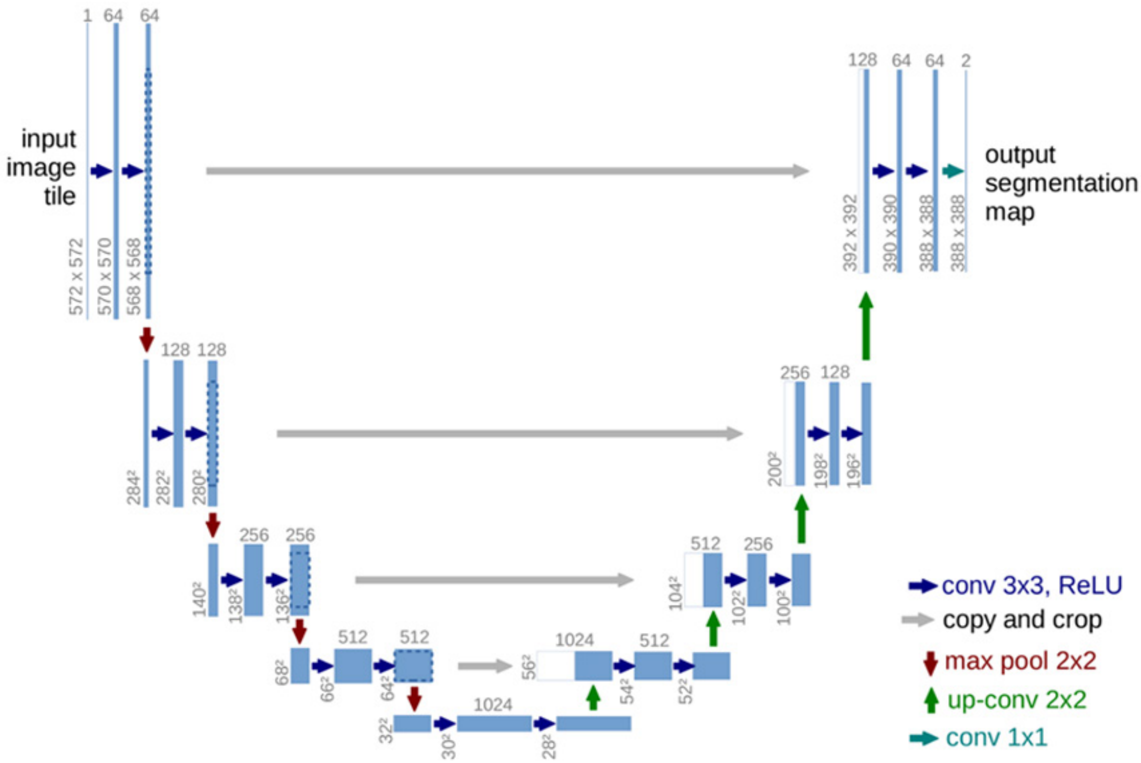

Figure 2. The Fundamental Architecture of U-Net. This figure was cited from [18].

a contracting (encoder) path and an expansive (decoder) path. The encoder path captures contextual information through convolution and pooling layers that reduce spatial resolution, while the decoder path restores spatial dimensions using upsampling layers. A distinctive characteristic of U-Net is the use of skip connections, which link corresponding layers in the encoder and decoder paths. These connections preserve high-resolution features, helping to maintain detailed boundaries during reconstruction [19].

Given the limited availability of medical imaging data—often constrained by privacy regulations and high acquisition costs-U-Net training typically involves data augmentation techniques such as rotation, scaling, and flipping. These strategies enhance dataset diversity, improve generalization, and promote the learning of robust feature representations [20]. The fundamental architecture of U-Net is shown in **Figure 2**.

In medical image processing, U-Net has demonstrated remarkable accuracy, supporting tasks such as early diagnosis, lesion monitoring, and treatment planning. Numerous U-Net variants have since been proposed to further improve segmentation performance. These variants generally fall into three categories:

Dimension-based variants

This category adapts the U-Net architecture to the dimensional characteristics of specific medical data.

3D U-Netis an extension of the classic U-Net, optimized for volumetric data [21]. It retains the symmetric encoder-decoder structure and skip connections but employs 3D convolutions to directly process three-dimensional inputs. Compared to its 2D counterpart, 3D U-Net more effectively captures spatial dependencies across multiple slices, resulting in improved segmentation accuracy for volumetric images.

V-Net, proposed by Milletari et al. in 2016, is another influential architecture tailored for 3D medical image segmentation, particularly under conditions of limited annotated data [22]. While structurally similar to U-Net, V-Net introduces several key innovations, most notably the Dice loss function, which effectively addresses class imbalance problems common in medical datas-

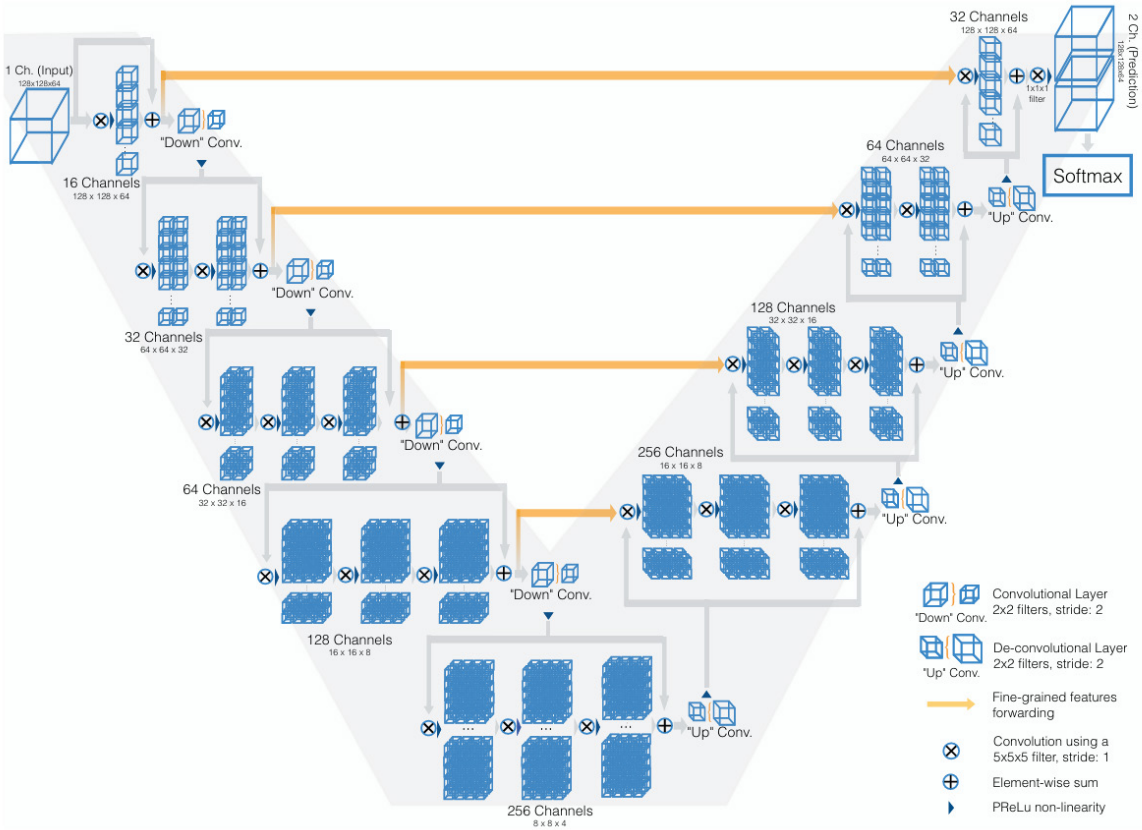

Figure 3. The Fundamental Architecture of the V-Net. This figure was cited from [22].

ets. The fundamental architecture of V-Net is shown in **Figure 3**.

Both 3D U-Net and V-Net represent important evolutions of the U-Net framework, offering powerful solutions for volumetric segmentation. These models have significantly advanced the field by enabling more accurate and efficient processing of complex three-dimensional medical images.

Structural optimization-based variants

This category improves segmentation performance by optimizing the internal architecture of the network. Techniques include the integration of residual connections, dense connectivity, and refined upsampling/downsampling strategies. A comparison of these architectural variants is presented in **Table 1**.

Residual U-Net, introduced by Zhang et al. in 2018, is inspired by ResNet, which was originally designed to address the vanishing gradient problem in deep neural networks [23, 24]. By integrating residual connections into the U-Net architecture, this variant enables deeper network structures while preserving input information. Specifically, residual blocks add input features directly to the output of convolution operations, mitigating information loss during training. This mechanism enhances both segmentation accuracy and computational efficiency, particularly in tasks requiring precise delineation of tissues, organs, and lesions.

Dense U-Net represents a more advanced evolution of the traditional U-Net, inspired by DenseNet [25]. It incorporates dense connectivity, where each layer receives inputs from all preceding layers, promoting gradient flow and improving feature propagation. Dense blocks within the encoder and decoder facilitate multi-scale feature reuse, reducing the number of parameters while enhancing representational power [26]. The architecture of Dense U-Net is shown in **Figure 4**.

U-Net++, proposed by Zhou et al. in 2018, further refines U-Net by introducing nested dense skip connections [27]. These connections form a series of subnetworks that allow deep supervision and multi-scale feature fusion. Each subnetwork connects to adjacent and all preceding

Table 1. Comparison of residual U-Net, dense U-Net, and nested U-Net

Methods	Basic Structure	Number of Parameters	Typical Clinical Scenario
Residual U-Net	U-Net + Residual Connections	High	General medical image segmentation
Dense U-Net	U-Net + Dense Connections	High	Segmentation tasks requiring rich feature reuse
Nested U-Net	U-Net + NestedSkip Connections	Low	Precise segmentation

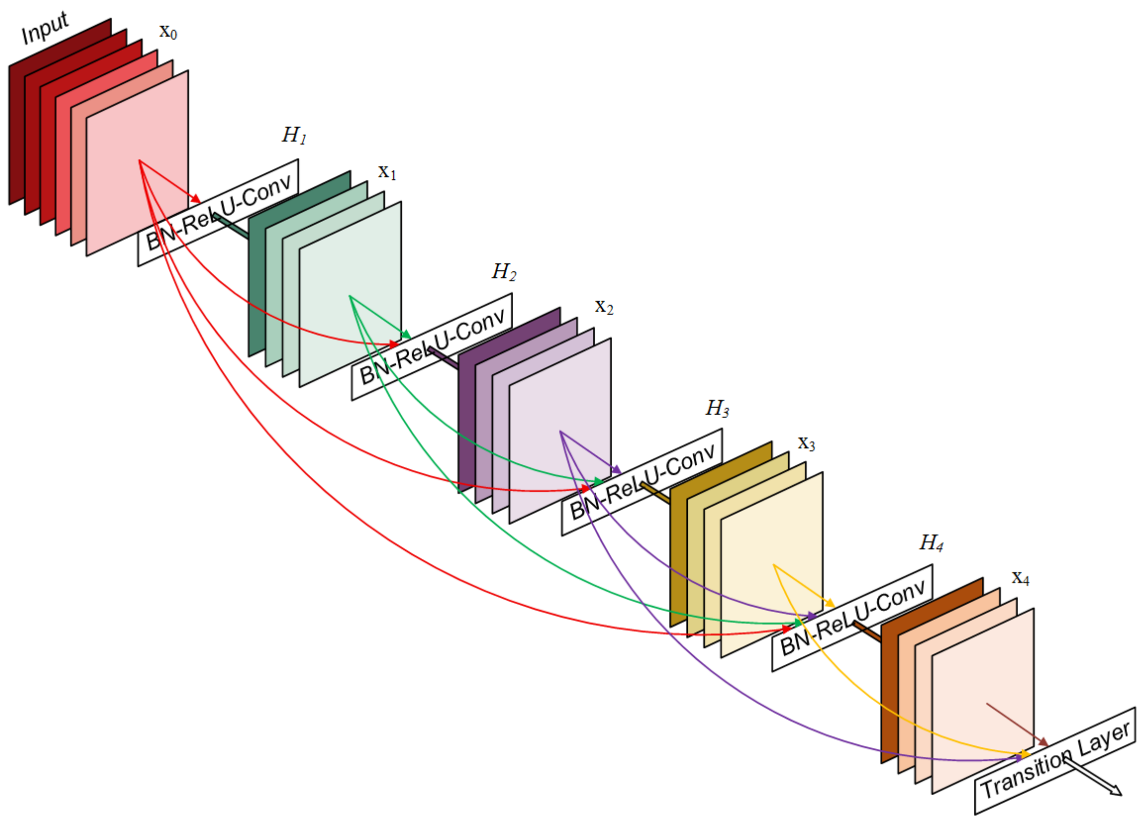

Figure 4. The Fundamental Architecture of Dense U-Net.

layers, improving the model's ability to capture structural details at various scales and reducing overfitting. U-Net++ is particularly effective in segmenting images with irregular morphologies and complex backgrounds, such as tumor delineation tasks [28]. A comparative analysis of Residual U-Net, Dense U-Net, and U-Net++ is summarized in **Table 1**.

Variants based on enhanced feature selection

This class of variants incorporates attention mechanisms to improve feature selection, allowing the network to focus on critical regions and ignore irrelevant information, thereby enhancing segmentation accuracy.

Attention U-Net, proposed by Oktay et al. in 2018, introduces attention gates into the encoder-decoder architecture [29]. These gates learn to highlight salient spatial regions during feature fusion, directing the network's focus toward informative areas while suppressing background noise. This mechanism improves segmentation performance in complex scenarios where target boundaries are unclear or embedded in heterogeneous backgrounds. The attention-enhanced architecture substantially increases model precision and efficiency across a range of medical imaging tasks.

Network architectures based on specialized designs

While U-Net has demonstrated exceptional performance in medical image segmentation, researchers have developed specialized archi-

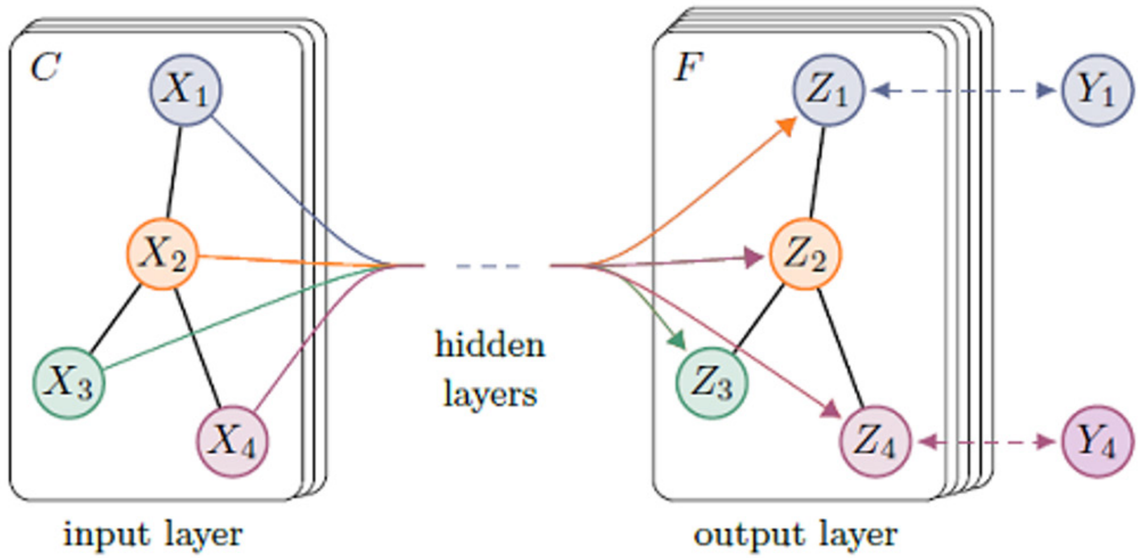

Figure 5. The Fundamental Architecture of GCN. GCN, graph convolutional network.

tectures to address its limitations in specific scenarios [30]. Compared with U-Net, these architectures offer improved generalization, robustness to limited data, enhanced structural feature extraction, and better integration of multimodal data—advantages particularly beneficial in ultrasound-guided regional anesthesia.

Architectures based on generative adversarial networks (GANs)

GANs consist of two components: a generator, which synthesizes data resembling the real distribution, and a discriminator, which distinguishes between real and generated samples. This adversarial training paradigm enables the generation of high-fidelity synthetic data or pseudo-labels, making GANs valuable in settings with scarce labeled data or high annotation costs.

Zhai et al. proposed an asymmetric semi-supervised GANs featuring two generators and one discriminator [31]. The two generators supervise each other, producing reliable segmentation masks even without labeled data, thereby enhancing model performance through the effective use of unlabeled samples. The method was evaluated on three public breast ultrasound datasets (DBUI, OASBUI, SPDBUI) and one additional dataset (SDBUI), demonstrating superior performance over fully and semi-supervised approaches under limited annotation conditions.

Architectures based on graph convolutional networks (GCNs)

GCNs extend convolution operations to non-Euclidean graph structures [32]. By leveraging neighborhood connectivity, GCNs update node features through information aggregation from neighboring nodes, effectively modeling complex spatial and semantic relationships. This capability enables GCNs to capture both local and global contextual information, which is particularly useful in processing images with irregular or non-grid structures [33].

In the context of neural blockade procedures, GCNs enhance the localization of nerve structures by modeling spatial dependencies, improving segmentation accuracy. The fundamental architecture of a GCNs is shown in **Figure 5**.

Ye et al. proposed a system that integrates segmentation and classification for breast cancer region of interest (ROI) images [34]. It comprises a segmentation module and a GCNs-based classification module. The segmentation module produces masks for image patches, which are merged to form the full ROI mask. The GCNs module constructs a graph using these patches, learning spatial and semantic relationships for classification. Extensive experiments confirmed the system's effectiveness and superior performance in breast cancer detection tasks.

Table 2. Comparison of GANs, GCNs, and multimodal architectures

Methods	Basic Structure	Data Type	Number of Parameters
GANs	Generator and a discriminator	Image data	High
GCNs	Convolutional layers	Graph-structured data	Variable (Graph-size dependent)
Multimodal Architectures	Combines multiple data modalities	Various	Variable

Note: GANs, generative adversarial networks; GCNs, graph convolutional networks; Multimodal Architectures, integrate heterogeneous data types to enhance model robustness.

Multimodal-based architecture

Multimodal medical image segmentation involves the integration of multiple imaging modalities to enhance anatomical and pathological interpretation, thereby improving segmentation accuracy [35]. Each modality offers unique strengths-CT provides high-resolution bone structure imaging, while MRI yields superior soft tissue contrast. By fusing such complementary information, multimodal approaches can overcome challenges such as low contrast, noise, and blurred boundaries, delivering more robust and reliable segmentation results [36].

One representative study proposed a multimodal segmentation network using the BraTS dataset to delineate brain tumors into three distinct regions: the whole tumor, the tumor core, and the enhancing tumor core [37]. The network accepts four MRI modalities (T1, T1c, T2, and FLAIR) as multi-channel input to construct a unified feature representation. Following the hierarchical anatomical structure of brain tumors, the network decomposes the complex multi-class segmentation task into sequential sub-tasks: segmenting the entire tumor, then the tumor core within the bounding box of the whole tumor, and finally the enhancing tumor core. Experimental results demonstrate significant improvements in segmentation accuracy.

By leveraging the complementary characteristics of diverse imaging modalities, this multimodal segmentation strategy improves the precision of complex pathological region delineation. It has shown notable success in applications involving brain tumors, liver tumors, and cardiac structures, offering valuable support for clinical decision-making and treatment planning. A comparison of GANs-, GCNs-, and multimodal-based architectures is presented in **Table 2**.

Application of DL in neural blockade segmentation

Neural blockade involves interrupting nerve signal transmission via local anesthetic injection to induce analgesia or anesthesia [38]. Precise neural blockade relies on accurate localization of neural structures and injection sites, which enhances therapeutic efficacy and minimizes complications [39]. Under ultrasound guidance, real-time segmentation of neural structures is essential. Recent advances in DL, particularly CNNs, have introduced powerful tools for improving the precision and efficiency of neural blockade segmentation.

Applications in the upper limb

Brachial plexus block

Brachial plexus block is a regional anesthesia technique that anesthetizes the upper limb by blocking the brachial plexus nerve conduction pathway. It is widely used in upper extremity surgeries, trauma interventions, and chronic pain management. The success of this procedure depends heavily on the accurate localization of the brachial plexus to ensure effective anesthetic delivery and avoid complications.

Wang et al. developed BPSegSys, a DL-based system for brachial plexus segmentation [40]. A total of 320 ultrasound images of the brachial plexus from the intermuscular sulcus were collected and manually annotated. A novel loss function combining hinge loss and cross-entropy loss was proposed. The enhanced ATU-Net was trained on both original and augmented images, with periodic parameter validation to retain the model with the highest Intersection over Union (IoU). The results showed that BPSegSys consistently produced accurate segmentations, with IoU scores slightly exceeding those of expert clinicians. The system enables

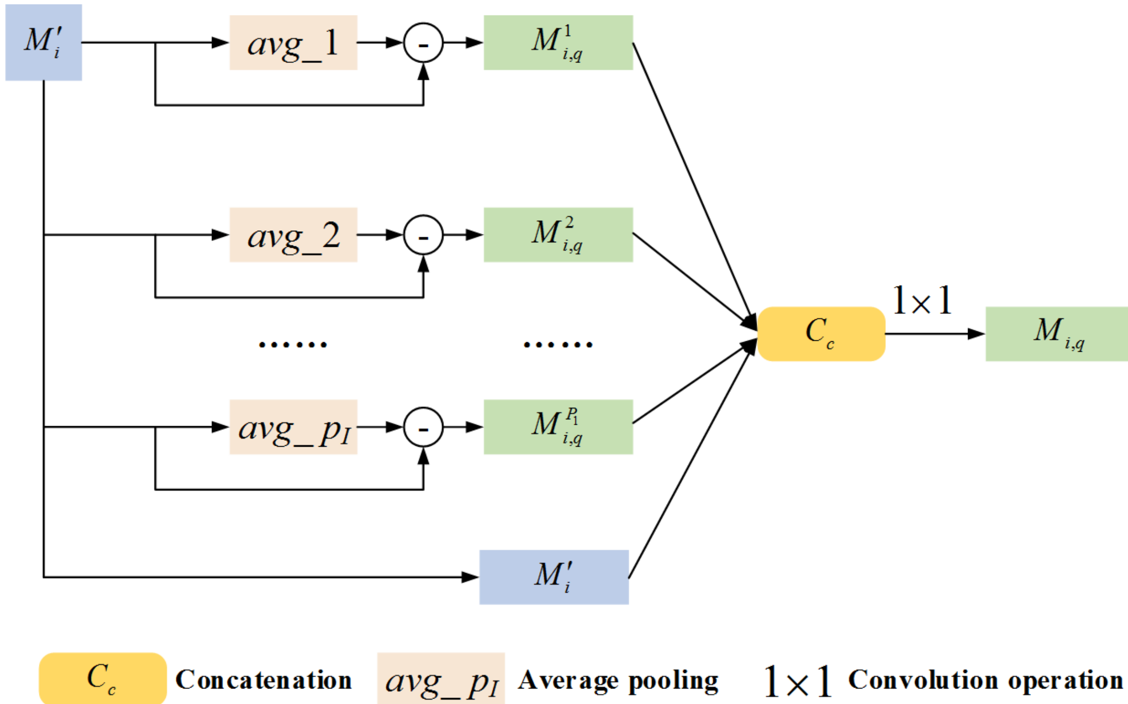

Figure 6. Pyramid edge extraction module. This figure was cited from [43].

segmentation of individual nerve trunks rather than general nerve block regions, thereby improving both accuracy and clinical efficiency.

Tian et al. evaluated multiple DL models for brachial plexus segmentation from ultrasound images [41]. Using a newly constructed dataset of 340 images labeled by three clinicians, they compared 12 models, including FCNs, SegNet, U-Net, and others. U-Net achieved the highest segmentation accuracy but was limited to processing 15 images per second due to its large model size. In contrast, LinkNet achieved the second-best accuracy while processing 142 images per second, indicating a favorable balance between accuracy and speed for real-time applications.

Ding et al. proposed MallesNet, a novel network designed for segmenting multiple anatomical structures—including nerves, arteries, veins, and muscles—in ultrasound images [42]. Using the UBPD dataset (1,055 images), MallesNet incorporated a Selective Local Contrast Feature module to extract multi-scale contrast features and a Spatial Attention Gate module to enhance channel-wise attention. Improved upsampling using transposed convolution and skip concatenation refined the final segmentation. MallesNet outperformed other methods in delineating neural and surrounding structures. The Pyramid Edge Extraction Module is illustrated in **Figure 6**.

Rayachoti et al. introduced the Ebola U-Net (EU-Net), a CNN-based model designed to address the limitations of U-Net in handling complex datasets [43]. EU-Net enhances feature extraction using bilateral filtering and a Pyramid Edge Extraction Module, with the Epidemic Optimization Algorithm employed for further refinement. Evaluated on four datasets—including the brachial plexus-EU-Net achieved 97.33% accuracy, a 1.36 RMSE, and a Dice coefficient of 94.97%, demonstrating high segmentation performance.

Huang et al. developed a hybrid attention network that employs pseudo-color enhancement for improved ultrasound segmentation [44]. By combining a pseudo-color enhancement algorithm with hybrid attention mechanisms, the model enhances long-range dependency modeling. The Multi-scale Channel Attention decoder efficiently utilizes encoder features, resulting in improved segmentation of brachial plexus, breast lesions, hemangiomas, and vaginal ultrasound images, as indicated by higher Dice metrics.

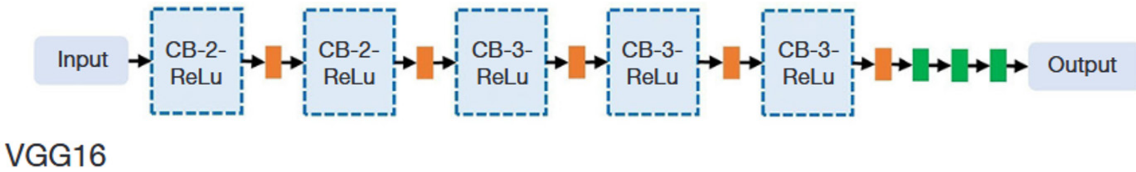

Figure 7. VGG16 network. This figure was cited from [48].

Zhou et al. proposed LAEDNet, a lightweight encoder-decoder network for ultrasound segmentation [45]. LAEDNet uses EfficientNet as the encoder and incorporates Lightweight Residual Squeeze-and-Excitation modules in the decoder. Available in three sizes (S, M, L), the model balances accuracy and computational cost. LAEDNet outperformed U-Net variants on CT datasets of the brachial plexus, breast, and fetal head circumference. The medium version, LAEDNet-M, achieved Dice scores of 73.0%, 73.8%, and 91.3% respectively, while maintaining a frame rate of 40.7 FPS, making it highly suitable for real-time clinical applications.

Median nerve block

The median nerve block is a regional anesthesia technique commonly used for procedures involving the hand, forearm, and wrist. It provides analgesia by inhibiting median nerve conduction and is widely applied in surgical interventions, trauma management, and chronic pain therapy.

Wang et al. proposed a deep similarity learning model, MNT-DeepSL (Median nerve tracking - deep similarity learning), for tracking the median nerve in carpal tunnel ultrasound images to aid in the diagnosis of carpal tunnel syndrome [46]. Traditional electrodiagnostic tests are costly, time-consuming, and lack standardized benchmarks, whereas ultrasound imaging offers a non-invasive, cost-effective alternative, with reported sensitivity and specificity of 94% and 98%, respectively. MNT-DeepSL integrates input decision rules, image representation, a difference layer, and ResNet. Across six wrist movement patterns, the model achieved over 90% tracking accuracy, especially during transitions such as from hook fist to full fist. This model provides precise localization of the median nerve in dynamic ultrasound sequences, enabling efficient and reliable tracking across various wrist positions, and offering a promising approach for rapid carpal tunnel syndrome screening.

Shao et al. assessed an improved U2-Net model for segmenting ultrasound images of the median nerve [47]. A total of 402 images were used, including 249 from carpal tunnel syndrome patients and 153 from healthy volunteers. Evaluation metrics included the Dice coefficient, pixel accuracy, and average Hausdorff distance. The improved U2-Net achieved a Dice score of 72.85%, mean IoU of 79.66%, and pixel accuracy of 95.92%, significantly outperforming conventional U-Net and Res-U-Net models. These findings demonstrate the enhanced segmentation performance of the improved U2-Net and its potential utility for early carpal tunnel syndrome diagnosis. The architecture based on the VGG (Visual Geometry Group) 16 network is illustrated in **Figure 7**.

Huang et al. developed an enhanced VGG16-UNet architecture incorporating a contracting path and an expanding path [48]. The contracting path employs a VGG16 backbone with the fully connected layers removed, while the expanding path mirrors the upsampling structure of U-Net. By integrating attention mechanisms and residual modules, several variants—A-UNet, S-UNet, and AS-UNet—were proposed and tested on 910 median nerve images. Results showed that AS-UNet achieved the best performance among U-Net-based models, while VGG16-UNet variants outperformed standard U-Net. Among these, attention-based architectures consistently outperformed residual-based ones, with A-VGG16-UNet delivering the highest accuracy, improving visualization of the median nerve and reducing the risk of iatrogenic injury to adjacent vessels and nerves.

Wu et al. evaluated multiple DL models pretrained on ImageNet, including DeepLabV3+, U-Net, FPN (Feature Pyramid Network), and Mask R-CNNs (Mask Region-based Convolutional Neural Networks), for automatic segmentation of the median nerve in dynamic ultrasound images [49]. U-Net, DeepLabV3+, and FPN were employed for semantic segmentation, while Mask R-CNNs was used for instance segmentation. Results indicated that DeepLabV3+ and Mask R-CNNs provided the best performance, with average IoU scores approaching 0.83, significantly improving the accuracy of nerve localization.

Horng et al. proposed a novel convolutional neural network, DeepNerve, for localizing and segmenting the median nerve in ultrasound video sequences [50]. The DeepNerve model comprises a convolutional layer, pooling layer, two fully connected layers, and a softmax layer. By incorporating spatial-temporal consistency techniques with CNNs, the model effectively reduces false positives caused by ultrasound image noise. It was evaluated on ultrasound sequences from 20 patients, each containing 400-600 frames, using cross-validation. Segmentation performance was primarily assessed by Dice coefficient and Hausdorff distance. Results demonstrated that DeepNerve outperformed both traditional CNNs and support vector machine (SVM) methods in nerve localization and segmentation, achieving superior accuracy.

Ulnar nerve block

Ulnar nerve block is an effective regional anesthesia technique for controlling pain in the hand and medial forearm. It is particularly suitable for surgical procedures and pain management in areas such as the wrist, elbow, and hand, including trauma repair.

Smistad et al. investigated the real-time segmentation of blood vessels, nerves, and bones during regional anesthesia using DL applied to ultrasound guidance [51]. The primary objective was to develop a system that assists non-expert users in interpreting ultrasound images, particularly for performing nerve blocks, by enabling real-time anatomical segmentation. The study collected 108 axillary ultrasound videos from healthy volunteers and patients, with annotations for the musculocutaneous, median, and ulnar nerves, and an additional 20 groin ultrasound videos for femoral nerve labeling. A U-Net architecture was applied with 10-fold cross-validation. For axillary nerve blocks, F1 scores for the musculocutaneous, median, and ulnar nerves were 0.72, 0.84, and 0.54, respectively. For femoral nerve blocks, the F1 scores for the femoral nerve, vascular structures, and bones were 0.79, 0.90, and 0.78, respectively. These findings demonstrate the potential of DL-based segmentation in enhancing the accuracy and efficiency of ultrasound-guided regional anesthesia, particularly for less experienced users.

Jimenez et al. proposed a method for automatic neural structure segmentation in ultrasound images using Random Under-Sampling (RUS) and SVM classifiers [52]. First, the ROI was defined using graph-cut-based techniques. The Simple Linear Iterative Clusteringalgorithm was then applied to divide the ROI into superpixels. Relevant features were extracted using a non-linear wavelet transform. Finally, classification was performed using RUS and SVM-based schemes to label each parameterized "hyperpixel", addressing the class imbalance between neural and non-neural regions. The dataset included 38 ultrasound images, with 22 depicting the median nerve and 16 depicting the ulnar nerve. Four classification approaches were compared: Gaussian Process Classifier, standard SVM, RUS-free SVM, and Weighted Lagrange Twin Support Vector Machine. Segmentation performance was assessed using the Dice coefficient and Geometric Mean. Results showed that the RUS-SVM method outperformed the other baselines, effectively identifying neural structures and providing technical support for peripheral nerve block applications. A comparison of medical image segmentation algorithms for upper limb nerve blocks is presented in **Table 3**.

Application in lower limbs

Lumbar plexus block

The lumbar plexus block is a commonly used anesthesia technique for lower limb surgeries and pain management. It involves injecting local anesthetics to block the lumbar plexus, resulting in partial or complete sensory and motor loss in the lower limb. Ultrasound guidance enhances the accuracy of this technique by providing real-time visualization of nerves and surrounding anatomy, thereby reducing the risk of complications.

Berggreen et al. employed a U-Net architecture to identify the femoral nerve in high-resolution ultrasound images, significantly improving visualization accuracy essential for precise nerve blocks [53]. Built using the TensorFlow frame-

Table 3. Comparison of medical image segmentation algorithms for upper limb nerve blockade

Nerve Type	Author	Model/Method	Core Innovation
Brachial Plexus	Wang et al. [40]	BPSegSys	Hybrid loss (hinge + cross-entropy) driven attention U-Net
	Tian et al. [41]	Multi-model comp.	LinkNet balances accuracy (Dice: 0.85) and speed (142 FPS)
	Ding et al. [42]	MallesNet	Multi-target segmentation + SLCF module for small objects
	Rayachoti et al. [43]	EU-Net	Pyramid Edge Extraction Module edge extraction + EOA optimization (Dice: 94.97%)
	Huang et al. [44]	HybridAttNet	Pseudo-color enhancement + MSCA decoder
	Zhou et al. [45]	LAEDNet	EfficientNet encoder + Lightweight Residual Squeeze-and-Excitation module (40.7 FPS)
Median Nerve	Wang et al. [46]	MNT-DeepSL	ResNet-based tracking (accuracy >90%)
	Shao et al. [47]	U2-Net+	Architecture optimization (Dice: 72.85%)
	Huang et al. [48]	AS-UNet	VGG16-UNet + attention fusion
	Wu et al. [49]	Mask R-CNNs	Pretrained instance segmentation (IoU: 0.83)
	Horng et al. [50]	DeepNerve	Spatiotemporal CNNs (Dice: 0.81, HD: 1.2 mm)
	Smistad et al. [51]	Real-time U-Net	Multi-structure segmentation (F1: 0.54-0.84)
	Jimenez et al. [52]	RUS-SVM	Graph-cut + imbalanced classification (Dice coefficient: 0.78)

Note: SLCF, Small Lesion Context Fusion; EOA, Edge Optimization Algorithm; EU-Net, Ebola U-Ne; MSCA, Multi-Scale Context Attention; CNNs, Convolutional Neural Networks; RUS-SVM, Random Under-Sampling-Support Vector Machine; HD, Hausdorff Distance.

work, the model utilized the Adam optimizer and categorical cross-entropy loss. A dataset of 1,410 ultrasound images from 48 patients was manually annotated by clinical experts. After 350 training epochs and 10-fold cross-validation, the model achieved an IoU score of 74%, indicating strong performance. The study also examined the influence of demographic variables such as height, weight, age, and BMI through t-tests and chi-square analysis. Results confirmed that DL-based semantic segmentation using U-Net can accurately segment the femoral nerve even with limited training data.

Similarly, Huang et al. applied a U-Net model to a dataset of 562 ultrasound images [54]. The training, validation, and test sets achieved IoU scores of 0.713, 0.633, and 0.638, respectively. The model attained an overall accuracy of 88.4%, demonstrating satisfactory performance and potential for clinical adoption.

Hong et al. explored image reconstruction, processing, and analysis using data-driven and AI techniques [55]. Focusing on knee ligament reconstruction and femoral arteriography, they proposed a constrained data exploration method combined with an iterative algorithm to reconstruct high-resolution images from low-frequency K-space data. Simulated experiments using enhanced images of knee ligaments and femoral nerve arteriography supported the approach. A multi-input segmentation network was designed to leverage the spatial continuity of knee ligaments and femoral nerves. The multi-supervision output yielded excellent segmentation results, providing clinically valuable information for pain management.

Smistad et al. developed a novel algorithm in 2016 for real-time automatic detection of the femoral artery [56]. **Figure 8** shows a segmented and visualized ultrasound image of the femoral artery using the FAST (Framework for Heterogeneous Medical Image Computing and Visualization) framework. The algorithm models the artery as an ellipse and assigns an ellipse score to each pixel. The best-scoring ellipse is selected as the arterial candidate, and a Kalman filter is applied for robust tracking under noisy and dynamic conditions. The algorithm also includes anatomical registration to align real-time ultrasound images with known anatomical structures, improving visualization accuracy.

Building on this, a subsequent study introduced a real-time automatic segmentation and

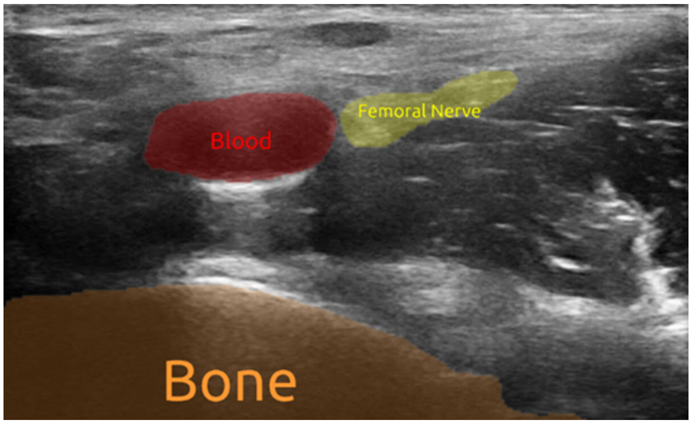

Figure 8. Example of an ultrasound femoral image segmented and visualized in real-time with FAST. This figure was cited from [57].

probe guidance system for ultrasound-guided femoral nerve blocks [57]. Utilizing modern GPUs (Graphics Processing Units) and the FAST framework, the system segments the femoral artery, femoral nerve, and fascial layers (fascia lata and fascia iliaca) in real time. Segmentation accuracy improved significantly, with positional errors between 1 and 3 mm and an average deviation of 8.5 mm from expert annotations. The system also featured transparent probe visualization and dynamic indicator updates, helping clinicians intuitively interpret ultrasound images. The study concluded that such computer-assisted tools are clinically feasible and may enhance success rates in femoral nerve blocks.

Accurate segmentation of the lumbosacral plexus is crucial for diagnosing and analyzing nerve injuries. While many DL models for spinal segmentation exist, they mainly focus on vertebrae and intervertebral discs rather than neural structures. Zhao et al. addressed this by proposing RA2-Net, a Residual Attention Network designed specifically for lumbosacral plexus segmentation [58]. RA2-Net consists of three key components: (1) an atrous encoder module that extracts multi-scale contextual features from MRI; (2) residual skip connections that merge high-resolution encoder features with high-level decoder outputs; and (3) a scale attention block that fuses multi-scale features in the decoder. Evaluated on spinal MR images from 10 patients, RA2-Net outperformed several state-of-the-art methods in segmenting the lumbosacral plexus.

Sciatic nerve block

The sciatic nerve block is commonly used in foot, ankle, and knee surgeries. To achieve complete anesthesia of the lower extremity, it is often combined with a femoral nerve block. This combined approach provides comprehensive coverage of the lower limb's sensory regions, making it suitable for extensive procedures involving the thigh, knee, and areas below.

Jimenez-Castaño et al. proposed a method using Random Fourier Features (RFF) to enhance ultrasound image segmentation of peripheral nerves via DL [59]. This method improved three semantic segmentation architectures—FCNs, U-Net, and ResUnet—by integrating RFF, resulting in RFF-FCNs, RFF-U-Net, and RFF-ResUnet. Two ultrasound datasets, Nerve UTP and NSD, were used, including images of the sciatic, ulnar, median, and femoral nerves. Results showed that RFF integration improved generalization in nerve segmentation. On the Nerve UTP dataset, RFF-FCNs and RFF-U-Net improved segmentation accuracy in most cases, although ResUnet and RFF-ResUnet experienced overfitting. On the NSD dataset, RFF-U-Net yielded the best segmentation results. This approach demonstrates strong potential for enhancing peripheral nerve segmentation while maintaining interpretability.

Díaz-Vargas et al. developed a variant of the U-Net, termed Conditional U-Net (C-U-Net), for improved automatic segmentation of peripheral nerves in ultrasound images [60]. By introducing a conditional input at the network's bottleneck to specify the target nerve type, the model learns structure-specific features, enhancing segmentation accuracy. Trained on a dataset comprising images of the sciatic, ulnar, median, and femoral nerves, C-U-Net outperformed the conventional U-Net. On 372 validation images, it achieved an average Dice coefficient of 0.70, accuracy of 0.73, sensitivity of 0.71, and an AUC of 0.85. These findings suggest that incorporating target-specific information significantly enhances model performance in multi-nerve ultrasound segmentation.

Sugino et al. investigated optimal scaling of network architectures and input image sizes for ultrasound-guided nerve block detection using CNNs [61]. The study focused on pixel-level labeling via deep CNNs, comparing an encoder-decoder model based on U-Net with a twostage model based on Mask R-CNNs. Both models performed well in nerve segmentation tasks. Two datasets were employed to examine the impact of model size and input resolution on performance. The public dataset contained 600 ultrasound images of the sciatic, ulnar, femoral, and median nerves. Results showed that smaller input sizes combined with larger network models significantly enhanced detection accuracy. A key finding was that optimized configurations not only improved precision but also enabled real-time processing, highlighting potential for clinical implementation in nerve localization during regional anesthesia.

Popliteal nerve block

The popliteal nerve block targets the sciatic nerve in the lower limb to provide anesthesia and analgesia below the knee. It is commonly applied in procedures involving the foot, ankle, and Achilles tendon.

Kawanishi et al. aimed to develop a DL algorithm to assess tibial nerve tension across different ankle positions [62]. The study used 204 ultrasound images from 68 healthy volunteers, covering maximum dorsiflexion and plantarflexion angles at -10° and -20°. The tibial nerve was manually segmented and subsequently classified using U-Net and a CNNs. Manual segmentation achieved an average maximum accuracy of 0.92, while the fully automated classification reached an accuracy of over 0.77, demonstrating feasibility in assessing nerve tension at varying ankle angles. The study noted the clinical potential of ultrasound imaging for screening but acknowledged limitations such as small sample size and variability in ultrasound device performance.

Kolluru et al. developed NerveTracker, a Python-based tool for visualizing and tracking peripheral nerve fibers using tandem block-face microscopy [63]. This approach integrates 3D microscopic imaging with UV surface excitation for high-resolution nerve imaging. A 2D U-Net-based segmentation model was designed for multi-class segmentation of 3D-MUSE image stacks, specifically targeting fascicles and epineurium. Pretrained weights from the ImageNet database were used to initialize the network, improving segmentation accuracy. Selective annotation (one out of every 100 slices) was applied during training, after which the model could automatically segment entire image stacks. The method demonstrated high accuracy in trajectory mapping for vagus and tibial nerves, with Dice similarity coefficients exceeding 0.75, and robustness across varying image characteristics.

A comparison of medical image segmentation algorithms for lower limb nerve blockade is presented in **Table 4**.

Discussion

The integration of DL with ultrasound imaging marks a significant advancement in the field of regional anesthesia, offering considerable potential to improve the accuracy and efficiency of peripheral nerve blockade. As demonstrated in numerous studies reviewed herein, DL algorithms—particularly those based on convolutional neural networks such as U-Net and its variants—have shown impressive capabilities in automatically segmenting peripheral nerves in complex ultrasound images. Clinically, this promises to reduce operator dependency, improve procedural consistency, enhance patient safety by minimizing the risk of inadvertent punctures, and streamline workflows by automating a previously time-intensive interpretation step.

However, realizing the full clinical potential of this technology involves challenges beyond achieving high segmentation accuracy in controlled environments. A major limitation is the robustness and generalizability of current DL models. Ultrasound image quality and characteristics can vary significantly due to factors such as machine vendors, imaging settings, operator skill, and patient-specific anatomy. As a result, models trained on curated datasets often struggle to maintain performance in diverse real-world scenarios. This variability currently limits the feasibility of a universal model applicable across all nerve types and clinical contexts. In the near term, developing specialized or adaptive models may offer a more practical solution.

Beyond technical and data-related constraints, significant challenges exist at the clinical translation interface. The implementation of AI-assisted guidance systems requires rigorous validation to meet regulatory standards. This includes demonstrating not only accuracy, but also safety, reliability, and clinical utility across

Table 4. Comparison of medical image segmentation algorithms for lower limb nerve blockade

Nerve Type	Author	Model/Method	Core Innovation
Lumbar Plexus	Berggreen et al. [53]	U-Net	High-precision femoral nerve segmentation (IoU: 74%) with demographic analysis
	Huang et al. [54]	U-Net	Multi-stage dataset validation (train/test IoU: 0.713/0.638)
	Hong et al. [55]	Data-driven + AI	Iterative reconstruction + multi-layer input segmentation network
	Smistad et al. [56]	Elliptical scoring	Femoral artery modeling + Kalman filter-based dynamic tracking
	Smistad* et al. [57]	GPU real-time system	Multi-structure segmentation (error: 1-3 mm) with probe guidance
	Zhao et al. [58]	RA2-Net	Residual-attention network + multi-scale fusion (lumbosacral MRI)
Sciatic Nerve	Jimenez-Castaño et al. [59]	RFF-enhanced models	RFF for FCNs/U-Net/ResUnet generalization
	Díaz-Vargas et al. [60]	C-UNet	Conditional U-Net with nerve-type input (Dice: 0.70)
	Sugino et al. [61]	Multi-scale CNNs	Image/model scaling optimization + real-time validation
Popliteal Nerve	Kawanishi et al. [62]	U-Net + CNNs	Tibial nerve tension analysis (accuracy: 0.77+) across ankle positions
	Kolluru et al. [63]	NerveTracker	3D microscopy + 2D U-Net (Dice >0.75) for nerve fascicle/epineurium segmentation

Note: RA2-Net, Residual Attention Adaptive Network; RFF, Random Fourier Features; C-Unet, Conditional U-Net; FCNs, Fully Convolutional Networks; MRI, Magnetic Resonance Imaging; CNNs, Convolutional Neural Networks; 3D, Three-Dimensional.

varied populations and healthcare settings—often necessitating large-scale, prospective clinical trials. Equally important is clinician trust and seamless integration into existing workflows. For AI to be adopted widely, it must offer user-friendly interfaces, transparent decision-making processes, and tangible benefits without disrupting established clinical practices or contributing to skill degradation. Integration with existing ultrasound systems and hospital information infrastructures is also essential but often underestimated.

Moreover, ethical considerations must guide the development and deployment of these technologies. Ensuring patient data privacy and security throughout the AI lifecycle is non-negotiable. Responsible innovation in this field demands early and ongoing engagement with ethical principles, particularly when handling sensitive health information or making clinical recommendations.

Looking forward, several research priorities must be addressed to overcome these barriers. There is a need for models that are more robust to image variability and require less annotated data, potentially through techniques such as domain generalization, federated learning, or self-supervised learning. Developing lightweight, computationally efficient models that support real-time inference on portable ultrasound devices or edge hardware will be critical to enhancing accessibility. Additionally, the exploration of multimodal approaches could provide richer anatomical context, particularly in complex anatomical scenarios [64]. Ultimately, the field may evolve toward personalized guidance systems that adapt to individual patient anatomy and predicted clinical outcomes, advancing the vision of precision medicine in regional anesthesia.

Conclusion

The application of DL in ultrasound-guided peripheral nerve block identification is transforming the field of anesthesiology. This review comprehensively summarizes recent progress in the use of ultrasound and medical image segmentation techniques for nerve block applications in the extremities. It begins by categorizing and introducing mainstream segmentation algorithms, followed by detailed examples of their application in clinical scenarios. Finally, the review analyzes the advantages and limitations of these technologies and discusses future directions for the development of AI-assisted ultrasound-guided nerve block systems.

Author contributions: Jiaxun Jiang: Responsible for the general framework design of the article, the planning and organization of the research direction, led the writing and editing of the literature review section, and participated in the discussion and writing of the research methodology section. Miao Zhou: Provided medically relevant theoretical support and was responsible for the collection and organization of literature. Liangqing Lin: Provides theoretical support for relevant parts of the development of ultrasound medicine. Haipo Cui: Corresponding Author: Led the revision of the article, participated in the final review and revision of the article, ensured that all authors' comments were integrated, and ultimately approved the article for submission. Long Liu: Provides theoretical support for relevant parts of the development of ultrasound medicine. Jiaen Wu: Participated in literature searches, provided experimental data support, and was responsible for producing some of the graphs. Zhaopen Zhou: Partial data collection and organization and production of partial tables.

References

[1] Helen L, O'Donnell BD, Moore E. Nerve localization techniques for peripheral nerve block and possible future directions. Acta Anaesthesiol Scand 2015;59(8):962-974.

[2] Verrill PJ. Principles and practice of regional anaesthesia. PAIN 1988;33(3):391.

[3] Wu L, Xin Y, Li S, et al. Cascaded Fully Convolutional Networks for automatic prenatal ultrasound image segmentation. 2017 IEEE 14th International Symposium on Biomedical Imaging (ISBI 2017) 2017;663-666.

[4] Norouzi A, Rahim MSM, Altameem A, et al. Medical Image Segmentation Methods, Algorithms, and Applications. IETE Tech Rev 2014;31(3):199-213.

[5] Rana M, Bhushan M. Machine learning and deep learning approach for medical image analysis: diagnosis to detection. Multimed Tools Appl 2022;1-39.

[6] Muthukrishnan R. Edge Detection Techniques For Image Segmentation. Int J Comput Sci Inf Technol 2011;3:259-267.

[7] Kaganami HG, Beiji Z. Region-Based Segmentation versus Edge Detection. Proceedings of the 2009 Fifth International Conference on Intelligent Information Hiding and Multimedia Signal Processing 2009;1217-1221.

[8] Otsu N. A Threshold Selection Method from Gray-Level Histograms. IEEE Trans Syst Man Cybern: Syst 1979;9(1):62-66.

[9] Cui H, Hu L, Chi L. Advances in Computer-Aided Medical Image Processing. Appl Sci 2023; 13(12):7079.

[10] Litjens G, Kooi T, Ehteshami Bejnordi B, et al. A Survey on Deep Learning in Medical Image Analysis. Med Image Anal 2017;42:60-88.

[11] Zhang S, Metaxas D. On the challenges and perspectives of foundation models for medical image analysis. Med Image Anal 2024;91: 102996.

[12] Wu R, Liu Y, Liang P, et al. H-vmunet: High-order Vision Mamba UNet for medical image segmentation. Neurocomputing 2025; 624:129447.

[13] Long J, Shelhamer E, Darrell T. Fully convolutional networks for semantic segmentation. 2015 IEEE Conference on Computer Vision and Pattern Recognition (CVPR) 2015;3431-3440.

[14] Huang Y, Xu H. Fully convolutional network with attention modules for semantic segmentation. Signal Image Video P 2021;15(5):1031-1039.

[15] Miao S, Piat S, Fischer P, et al. Dilated FCN for multi-agent 2D/3D medical image registration. Proceedings of the Thirty-Second AAAI Conference on Artificial Intelligence and Thirtieth Innovative Applications of Artificial Intelligence Conference and Eighth AAAI Symposium on Educational Advances in Artificial Intelligence 2018;32:575.

[16] Wang Z, Gao X, Wu R, et al. Fully automatic image segmentation based on FCN and graph cuts. Multimedia Syst 2022;28(5):1753-1765.

[17] Qian L, Huang H, Xia X, et al. Automatic segmentation method using FCN with multi-scale dilated convolution for medical ultrasound image. Visual Comput 2023;39(11):5953-5969.

[18] Ronneberger O, Fischer P, Brox T. U-Net: Convolutional Networks for Biomedical Image Segmentation. Medical Image Computing and Computer-Assisted Intervention – MICCAI 2015 2015;234-241.

[19] Singadkar G, Mahajan A, Thakur M, et al. Deep Deconvolutional Residual Network Based Automatic Lung Nodule Segmentation. J Digit Imaging 2020;33(3):678-684.

[20] Oyedotun OK, El Rahman Shabayek A, Aouada D, et al. Training Very Deep Networks via Residual Learning with Stochastic Input Shortcut Connections. Neural Inf Process 2017;23-33.

[21] Çiçek Ö, Abdulkadir A, Lienkamp SS, et al. 3D U-Net: Learning Dense Volumetric Segmentation from Sparse Annotation. Medical Image Computing and Computer-Assisted Intervention – MICCAI 2016 2016;424-432.
[22] Milletari F, Navab N, Ahmadi SA. V-Net: Fully Convolutional Neural Networks for Volumetric Medical Image Segmentation. 2016 Fourth International Conference on 3D Vision (3DV) 2016;565-571.
[23] Zhang Z, Liu Q, Wang Y. Road Extraction by Deep Residual U-Net. IEEE Geosci Remote Sens Lett 2018;15(5):749-753.
[24] He K, Zhang X, Ren S, et al. Deep Residual Learning for Image Recognition. 2016 IEEE Conference on Computer Vision and Pattern Recognition (CVPR) 2016;770-778.
[25] Iandola F, Moskewicz M, Karayev S, et al. DenseNet: Implementing Efficient ConvNet Descriptor Pyramids. arXiv - CS - Computer Vision and Pattern Recognition 2014.
[26] Zhang J, Zhang Y, Jin Y, et al. MDU-Net: multi-scale densely connected U-Net for biomedical image segmentation. Health Inf Sci Syst 2023;11(1):13.
[27] Zhou Z, Rahman Siddiquee MM, Tajbakhsh N, et al. UNet++: A Nested U-Net Architecture for Medical Image Segmentation. arXiv - CS - Computer Vision and Pattern Recognition 2018.
[28] Gab Allah AM, Sarhan AM, Elshennawy NM. Edge U-Net: Brain tumor segmentation using MRI based on deep U-Net model with boundary information. Expert Syst Appl 2023;213: 118833.
[29] Oktay O, Schlemper J, Folgoc L, et al. Attention U-Net: Learning Where to Look for the Pancreas. arXiv - CS - Computer Vision and Pattern Recognition 2018.
[30] Egger J, Gsaxner C, Pepe A, et al. Medical deep learning—A systematic meta-review. Comput Meth Prog Bio 2022;221:106874.
[31] Zhai D, Hu B, Gong X, et al. ASS-GAN: Asymmetric semi-supervised GAN for breast ultrasound image segmentation. Neurocomputing 2022;493:204-216.
[32] Hou J, Wei H, Liu B. iPiDA-GCN: Identification of piRNA-disease associations based on Graph Convolutional Network. PLoS Comput Biol 2022;18(10):e1010671.
[33] Tian F, Tian Z, Chen Z, et al. Surface-GCN: Learning interaction experience for organ segmentation in 3D medical images. Med Phys 2023;50(8):5030-5044.
[34] Ye H, Wang DH, Li J, et al. Improving Histopathological Image Segmentation and Classification using Graph Convolution Network. Proceedings of the 2019 8th International Conference on Computing and Pattern Recognition 2020;192-198.
[35] Azam MA, Khan KB, Salahuddin S, et al. A review on multimodal medical image fusion: Compendious analysis of medical modalities, multimodal databases, fusion techniques and quality metrics. Comput Biol Med 2022;144: 105253.
[36] Wang X, Li Z, Huang Y, et al. Multimodal medical image segmentation using multi-scale context-aware network. Neurocomputing 2022; 486:135-146.
[37] Wang G, Li W, Ourselin S, et al. Automatic Brain Tumor Segmentation Using Cascaded Anisotropic Convolutional Neural Networks. Brainlesion: Glioma, Multiple Sclerosis, Stroke and Traumatic Brain Injuries 2018;178-190.
[38] Asher Y. Hadzic's Peripheral Nerve Blocks and Anatomy for Ultrasound-guided Regional Anesthesia, Second Edition. Anesthesiology 2013; 119:493-493.
[39] Sinha A, Chan VW. Ultrasound imaging for popliteal sciatic nerve block. Reg Anesth Pain Med 2004;29(2):130-134.
[40] Wang Y, Zhu B, Kong L, et al. BPSegSys: A Brachial Plexus Nerve Trunk Segmentation System Using Deep Learning. Ultrasound Med Biol 2024;50(3):374-383.
[41] Tian D, Zhu B, Wang J, et al. Brachial Plexus Nerve Trunk Recognition From Ultrasound Images: A Comparative Study of Deep Learning Models. IEEE Access 2022;10:82003-82014.
[42] Ding Y, Yang Q, Wang Y, et al. MallesNet: A multi-object assistance based network for brachial plexus segmentation in ultrasound images. Med Image Anal 2022;80:102511.
[43] Rayachoti E, Vedantham R, Gundabatini SG. EU-net: An automated CNN based ebola U-net model for efficient medical image segmentation. Multimed Tools Appl 2024;83(30):74323-74347.
[44] Huang X, Wang Q, Chen J, et al. Effective hybrid attention network based on pseudo-color enhancement in ultrasound image segmentation. Image Vision Comput 2023;137:104742.
[45] Zhou Q, Wang Q, Bao Y, et al. LAEDNet: A Lightweight Attention Encoder–Decoder Network for ultrasound medical image segmentation. Comput Electr Eng 2022;99:107777.
[46] Wang YW, Chang RF, Horng YS, et al. MNT-DeepSL: Median nerve tracking from carpal tunnel ultrasound images with deep similarity learning and analysis on continuous wrist mo-

tions. Comput Med Imaging Graph 2020; 80:101687.

[47] Shao J, Zhou K, Cai YH, et al. Application of an Improved U2-Net Model in Ultrasound Median Neural Image Segmentation. Ultrasound Med Biol 2022;48(12):2512-2520.

[48] Huang A, Jiang L, Zhang J, et al. Attention-VGG16-UNet: a novel deep learning approach for automatic segmentation of the median nerve in ultrasound images. Quant Imaging Med Surg 2022;12(6):3138-3150.

[49] Wu CH, Syu WT, Lin MT, et al. Automated Segmentation of Median Nerve in Dynamic Sonography Using Deep Learning: Evaluation of Model Performance. Diagnostics (Basel) 2021; 11(10):1893.

[50] Horng MH, Yang CW, Sun YN, et al. DeepNerve: A New Convolutional Neural Network for the Localization and Segmentation of the Median Nerve in Ultrasound Image Sequences. Ultrasound Med Biol 2020;46(9):2439-2452.

[51] Smistad E, Lie T, Johansen KF. Real-time segmentation of blood vessels, nerves and bone in ultrasound-guided regional anesthesia using deep learning. 2021 IEEE International Ultrasonics Symposium (IUS) 2021;1-4.

[52] Jimenez C, Diaz D, Salazar D, et al. Nerve Structure Segmentation from Ultrasound Images Using Random Under-Sampling and an SVM Classifier. Image Anal Recognit 2018;571-578.

[53] Berggreen J, Johansson A, Jahr J, et al. Deep Learning on Ultrasound Images Visualizes the Femoral Nerve with Good Precision. Healthcare (Basel) 2023;11(2):184.

[54] Huang C, Zhou Y, Tan W, et al. Applying deep learning in recognizing the femoral nerve block region on ultrasound images. Ann Transl Med 2019;7(18):453.

[55] Hong G, Zhang L, Kong X, et al. Artificial Intelligence Image-Assisted Knee Ligament Trauma Repair Efficacy Analysis and Postoperative Femoral Nerve Block Analgesia Effect Research. World Neurosurg 2021;149:492-501.

[56] Smistad E, Lindseth F. Real-Time Automatic Artery Segmentation, Reconstruction and Registration for Ultrasound-Guided Regional Anaesthesia of the Femoral Nerve. IEEE Trans Med Imaging 2016;35(3):752-761.

[57] Smistad E, Iversen DH, Leidig L, et al. Automatic Segmentation and Probe Guidance for Real-Time Assistance of Ultrasound-Guided Femoral Nerve Blocks. Ultrasound Med Biol 2017;43(1): 218-226.

[58] Zhao J, Sun L, Zhou X, et al. Residual-atrous attention network for lumbosacral plexus segmentation with MR image. Comput Med Imaging Graph 2022;100:102109.

[59] Jimenez-Castaño CA, Álvarez-Meza AM, Aguirre-Ospina OD, et al. Random Fourier Features-Based Deep Learning Improvement with Class Activation Interpretability for Nerve Structure Segmentation. Sensors (Basel) 2021;21(22): 7741.

[60] Díaz-Vargas HM, Jimenez-Castaño CA, Cárdenas-Peña DA, et al. Peripheral Nerve Segmentation in Ultrasound Images Using Conditioned U-Net. Prog Artif Intell Pattern Recognit 2021;124-133.

[61] Sugino T, Onogi S, Oishi R, et al. Investigation of Appropriate Scaling of Networks and Images for Convolutional Neural Network-Based Nerve Detection in Ultrasound-Guided Nerve Blocks. Sensors (Basel) 2024;24(11):3696.

[62] Kawanishi K, Kakimoto A, Anegawa K, et al. Automatic Identification of Ultrasound Images of the Tibial Nerve in Different Ankle Positions Using Deep Learning. Sensors (Basel) 2023; 23(10):4855.

[63] Kolluru C, Joseph N, Seckler J, et al. Nerve-Tracker: a Python-based software toolkit for visualizing and tracking groups of nerve fibers in serial block-face microscopy with ultraviolet surface excitation images. J Biomed Opt 2024;29(7):076501.

[64] Li X, Ma S, Xu J, et al. TranSiam: Aggregating multi-modal visual features with locality for medical image segmentation. Expert Syst Appl 2024;237:121574.